

Relativistic analytical R -matrix theory for strong-field ionization

Michael Klaiber^{✉,*}, Karen Z. Hatsagortsyan^{✉,†} and Christoph H. Keitel[✉]
Max-Planck-Institut für Kernphysik, Saupfercheckweg 1, 69117 Heidelberg, Germany

 (Received 28 November 2022; accepted 31 January 2023; published 14 February 2023)

The analytical R -matrix (ARM) theory has been known for an efficient description of the Coulomb effects of the atomic core in strong-field ionization in the nonrelativistic regime. We generalize the ARM theory into the relativistic domain aiming at the application to strong-field ionization of highly charged ions in ultrastrong laser fields. Comparison with the relativistic Coulomb-corrected strong-field approximations (SFA) is provided, highlighting the advantages and disadvantages. The weakly relativistic asymptotics and its accordance with the nondipole Coulomb-corrected SFA are examined. As an example of a physical application of the relativistic ARM, the Coulomb enhancement of tunneling ionization probability for highly charged ions at the cutoff of the direct channel is discussed.

DOI: [10.1103/PhysRevA.107.023107](https://doi.org/10.1103/PhysRevA.107.023107)

I. INTRODUCTION

Advances in the experimental technique for high-resolution measurements of photoelectron and ion momentum distributions [1,2] allowed the recent extension of experimental investigations of strong-field ionization beyond the dipole regime [3–13]. The leading nondipole effect is the radiation pressure, which is responsible for the partitioning of the absorbed photon momentum between the photoelectron and the parent ion in strong-field ionization [3,14–19]. Interesting dynamical properties arise due to the interplay between Coulomb effects of the atomic core and the nondipole effects [4–6,20–26]. The nondipole theory has been developed for the interpretation of experimental results, including the strong-field approximation (SFA) [14,18,19,27–37], the numerical solution of the time-dependent Schrödinger equation (TDSE) [30,38,39], as well as the classical trajectory Monte Carlo (CTMC) simulations [12,40–42].

While presently strong laser fields up to the intensity of 10^{23} W/cm² are achievable [43], the relativistic regime of the laser-atom interaction in ultrastrong fields is far from deep experimental scrutiny. This is because the most interesting dynamics, including electron correlations, is expected when the atomic and laser fields are of the same magnitude. The latter necessitates dealing with an atomic system of highly charged ions (HCI), which are extremely difficult to handle experimentally. The pioneering experiment in this field by Moore *et al.* [44] more than 20 years ago at an intensity of 3×10^{18} W/cm²

has been followed by a series of fine experiments aimed at the observation of signatures of the atomic bound dynamics in the photoelectron momentum distribution (PMD) during the ionization process in external fields of relativistic intensity [45–53]. It was clearly shown that the drift of the electron induced by the laser magnetic field suppresses the usual electron correlation channel—the recollision, and related phenomena of high-order harmonic generation, above-threshold ionization, and nonsequential double ionization, see, e.g., Refs. [40,46,54]. However, it is still not clear whether specific electron correlations in the relativistic regime of strong-field ionization, such as shake-up, shake-off processes, collective tunneling, etc. [55], would exist at suppressed recollisions.

The workhorses of analytical investigations in strong-field physics, strong-field approximation (SFA) [56–58] and the quasi-classical imaginary time method (ITM) [59,60] have been generalized into the relativistic regime in Refs. [61,62] and [63–66], respectively. However, in the standard SFA, the influence of the Coulomb field of the atomic core is neglected in the electron continuum dynamics. This approximation is especially unsuitable in the case of HCI.

In the nonrelativistic regime the ITM has been improved to treat Coulomb field effects during ionization and the well-known quantitatively correct Perelomov-Popov-Terent'ev (PPT) ionization rates have been derived [67] (in the adiabatic regime also known as Ammosov-Delone-Krainov (ADK) rates [68]). The PPT theory uses the quasi-classical wave function for the description of the tunneling part of the electron wave packet through the nonadiabatic barrier formed by the laser and the atomic field. The continuum wave function is matched to the exact bound state [59,69], in this way removing the singularity in the phase of the quasi-classical wave function at the Coulomb center. The PPT theory does not address Coulomb effects during the photoelectron dynamics in the continuum. The latter is very important for the forming of various features of the photoelectron momentum distribution (PMD) and has been treated within different versions of the Coulomb-corrected SFA (CCSFA). The

*klaiber@mpi-hd.mpg.de

†k.hatsagortsyan@mpi-hd.mpg.de

Published by the American Physical Society under the terms of the Creative Commons Attribution 4.0 International license. Further distribution of this work must maintain attribution to the author(s) and the published article's title, journal citation, and DOI. Open access publication funded by the Max Planck Society.

simplest approach is the Coulomb-Volkov ansatz when the Volkov wave function [70] in the SFA matrix element is replaced by the Coulomb-Volkov wave function [71,72], which incorporates the asymptotic phase of the exact Coulomb continuum wave function into the phase of the Volkov state. While the Coulomb-Volkov approach can be formulated rigorously as an S -matrix expansion [73], it accounts for the coupling between the Coulomb and the laser field perturbatively, and the approach fails when the electron appears in the continuum after tunneling close to the atomic core [74].

The extension of the nonrelativistic PPT theory to treat the Coulomb effects in the continuum also employs the electron continuum wave function in the eikonal approximation [75–77]. The CCSFA via the eikonal approximation has been rigorously formulated in [78,79], evaluating the eikonal phase of the continuum electron wave function along the exact classical electron trajectories driven by the laser and the Coulomb field. The same approximation has been worked out in Refs. [80,81] via the Feynman path integration concept. Higher-order contributions in CCSFA have been discussed in Ref. [82] by removing the Coulomb singularity with the use of the saddle-point approximation [83] rather than with the matching procedure to the bound state.

An innovative way of matching the electron eikonal wave function for the continuum to the atomic bound state within the nonrelativistic SFA approach has been advanced in the analytical R -matrix (ARM) theory [84–87]. Here, it has been shown that the rigorous matching procedure is equivalent to a particular (imaginary) shift of the starting point of the complex time integration in the phase of the eikonal wave function in the SFA amplitude. The ARM theory provides the most efficient version of CCSFA. While the employed eikonal approximation in different versions of CCSFA allows the treatment of rescattering effects, it restricts the rescattering only to soft ones [88].

The relativistic regime of strong-field ionization can be characterized by the following parameters. For the subbarrier dynamics, the parameter $\nu \equiv \kappa/c \sim 1$ indicates the relativistic domain, with the atomic momentum $\kappa = \sqrt{2I_p}$, the ionization energy I_p , and the speed of light c . For the continuum dynamics, the relativistic domain is achieved when the relativistic invariant field parameter $\xi \equiv E_0/(c\omega) \sim 1$, with the laser field amplitude E_0 and the frequency ω . Recollisions in the relativistic regime are suppressed when the Lorentz deflection parameter $\Gamma_R \gtrsim 1$, with $\Gamma_R \equiv (1/16)\nu\xi^3(c^2/\omega)$ [40,89]. Atomic units are used throughout.

The relativistic domain of strong-field ionization is accessible with HCI driven by ultrastrong laser fields. The ITM including Coulomb corrections during ionization has been extended into the relativistic regime [63–66], allowing to calculate quantitatively relevant ionization rates in the relativistic case. The relativistic version of the plain SFA has been put forward by Reiss in Refs. [61,62]. The CCSFA, based on the relativistic eikonal-Volkov wave function for the continuum electron [90], has been proposed in Ref. [91]. The calculation of spin-resolved ionization probabilities in the relativistic regime using relativistic CCSFA has been provided in Ref. [92], showing the equivalence of the CCSFA to the Coulomb-corrected ITM.

We indicate also the significant efforts in the numerical investigations of the relativistic ionization dynamics via the Dirac equation, in particular with HCIs and superstrong laser fields, carried out in Refs. [93–105].

In this paper the ARM theory is extended into the relativistic domain aiming at the application of strong-field ionization of HCIs in ultrastrong laser fields. The ARM theory [84–87] is a version of the eikonal approximation in the description of the Coulomb field of the atomic core for the electron during its continuum dynamics after ionization in a strong laser field. The main advantage of the ARM theory is that the explicit matching procedure of the continuum wave function to the bound state is replaced by the specific shift of the border of the time integration into the complex plane in the eikonal. The consequence of this procedure is that the singularity of the wave function at the saddle point of the time integration (corresponding to the center of the Coulomb potential) is eliminated. For the extension of the ARM theory into the relativistic regime we make use of the latter property, namely, derive such a shift of the time integration border in the complex domain, which eliminates the singularity of the phase of the relativistic CCSFA wave function at the time saddle point. Finally, we apply the relativistic ARM theory for the investigation of the Coulomb enhancement effect at the cutoff of the direct ionization channel in the relativistic domain with HCIs. This effect is known in the nonrelativistic regime, described in Refs. [88,106].

The structure of the paper is the following. In Sec. II we begin with the nonrelativistic regime, elucidating our approach for the derivation of the ARM theory amplitude, then apply it for the relativistic case in Sec. III. Examples of the application of the derived relativistic ARM theory are discussed in Secs. IV–VI, and our conclusions are formulated in Sec. VII.

II. NONRELATIVISTIC THEORY

In this section we elucidate our approach for the derivation of the ARM-theory amplitude in the nonrelativistic regime. Note that the ionization amplitude in the nonrelativistic ARM theory has been derived in Refs. [84–87] by dividing the interaction region into two subregions (inner region and outer region), and by rigorously matching the eikonal wave function for the continuum electron in the outer region to the bound state wave function in the inner region using an R -matrix approach. Here, we use an operational approach, namely, taking into account that the above-mentioned matching procedure of the wave functions is equivalent to a shift of the time integration border in the complex domain, and we derive such a shift of the time integration border in the eikonal that eliminates the singularity of the SFA amplitude. Firstly, we derive with our operational approach the strong-field ionization amplitude in the case of a short-range atomic potential and then discuss the case with the Coulomb field.

We apply SFA for the description of the laser-driven ionization process of the atomic bound electron. The SFA ionization amplitude of the electron with asymptotic outgoing momentum \mathbf{p} is given by [107]

$$m_{\mathbf{p}} = -i \int dt \langle \psi_{\mathbf{p}}(t) | H_i(t) | \phi(t) \rangle, \quad (1)$$

where $\phi(t)$ is the bound state wave function, $\psi_{\mathbf{p}}(t)$ the electron outgoing continuum state, and the interaction Hamiltonian in the length gauge

$$H_i(t) = \mathbf{r} \cdot \mathbf{E}(t), \quad (2)$$

with the laser electric field $\mathbf{E} = -\partial_t \mathbf{A}$.

A. Short-range potential

Let us first derive the analytical expression of the ionization amplitude in the leading order E_0/E_a term in the case of a short-range atomic potential, where $E_a = \kappa^3$ is the atomic field. In this case the continuum state in the laser field in Eq. (1) is described by the Volkov state [70], $\psi_{\mathbf{p}}(\mathbf{r}, t) \rightarrow \psi_{\mathbf{p}}^{(0)}(\mathbf{r}, t)$:

$$\psi_{\mathbf{p}}^{(0)}(\mathbf{r}, t) = \frac{1}{\sqrt{(2\pi)^3}} \exp \left\{ i[\mathbf{p} + \mathbf{A}(t)] \cdot \mathbf{r} + i \int_t ds \frac{[\mathbf{p} + \mathbf{A}(s)]^2}{2} \right\}, \quad (3)$$

with the laser vector potential $\mathbf{A}(t)$; here we consider a linearly polarized laser field. The bound state in the case of the short-range potential is $\phi(\mathbf{r}, t) \rightarrow \phi^{(0)}(\mathbf{r}, t)$:

$$\phi^{(0)}(\mathbf{r}, t) = \sqrt{\frac{\kappa}{2\pi r^2}} \exp \left[-\kappa r + i \frac{\kappa^2}{2} t \right]. \quad (4)$$

In this case we straightforwardly arrive at the amplitude $m_{\mathbf{p}} \rightarrow m_{\mathbf{p}}^{(0)}$:

$$m_{\mathbf{p}}^{(0)} = -\frac{i\sqrt{\kappa}}{4\pi^2} \int d^3\mathbf{r} \int dt \frac{\mathbf{r} \cdot \mathbf{E}(t)}{r} \exp \left\{ -i[\mathbf{p} + \mathbf{A}(t)] \cdot \mathbf{r} - i \int_t ds \frac{[\mathbf{p} + \mathbf{A}(s)]^2}{2} + i \frac{\kappa^2}{2} t - \kappa r \right\}. \quad (5)$$

In the next step we approximate the t integration via the saddle-point approximation (SPA). Here the solution of the t -saddle-point equation,

$$[\mathbf{p} + \mathbf{A}(t)]^2 + \kappa^2 + 2\mathbf{r} \cdot \mathbf{E}(t) = 0, \quad (6)$$

is found perturbatively with respect to the last term, which is equivalent to an expansion in the parameter E_0/E_a . It yields

$$t_s = \tilde{t}_0 + i \frac{\mathbf{r} \cdot \mathbf{E}(\tilde{t}_0)}{|\mathbf{E}(\tilde{t}_0)|\tilde{\kappa}} \approx \tilde{t}_0 + i \frac{\mathbf{r} \cdot \mathbf{E}(t_0)}{|\mathbf{E}(t_0)|\kappa}, \quad (7)$$

where $\tilde{\kappa} = \sqrt{\kappa^2 + p_{\perp}^2}$, and \tilde{t}_0 is the common zeroth-order solution [108] via

$$[\mathbf{p} + \mathbf{A}(\tilde{t}_0)]^2 + \kappa^2 = 0. \quad (8)$$

Here, we distinguish between \tilde{t}_0 and $t_0 = \tilde{t}_0(\mathbf{p}_{\max})$, with $\mathbf{p}_{\max} = [0, A(t_{\max}), 0]$ the most probable quasi-classical momentum in the nonrelativistic case, corresponding to the ionization at the time t_{\max} . In the perturbation term in Eq. (7), we approximate $\tilde{\kappa} \approx \kappa$ and $\tilde{t}_0 \approx t_0$, because otherwise higher-order terms with respect to E_0/E_a would be included. Note that the time dependence of the preexponential in Eq. (5) $\partial_t \ln[E(t)] \sim \omega$ is small and can be neglected with an accuracy

of ω/I_p . With the solution Eq. (7), the amplitude in SPA yields

$$m_{\mathbf{p}}^{(0)} = -i \int d^3\mathbf{r} \mathcal{M}^{(0)}(\mathbf{r}), \quad (9)$$

$$\mathcal{M}^{(0)}(\mathbf{r}) = \frac{1}{4\pi^2} \sqrt{\frac{2\pi}{|\mathbf{E}(t_0)|}} \frac{\mathbf{r} \cdot \mathbf{E}(t_0)}{r} \times \exp \left\{ -i[\mathbf{p}_{\max} + \mathbf{A}(t_0)] \cdot \mathbf{r} - \frac{(\mathbf{r} \cdot \mathbf{E}(t_0))^2}{2\kappa|\mathbf{E}(t_0)|} - \kappa r - i \int_{t_0} ds \frac{1}{2} [\mathbf{p} + \mathbf{A}(s)]^2 + i \frac{\kappa^2}{2} \tilde{t}_0 \right\}, \quad (10)$$

where the terms up to the first order in E_0/E_a in the exponent are kept, and with the same accuracy, the prefactor is estimated at $\mathbf{p} = \mathbf{p}_{\max}$. The remaining \mathbf{r} integral is then calculated analytically:

$$m_{\mathbf{p}}^{(0)} = \frac{i}{\sqrt{2\pi} |\mathbf{E}(t_0)|} \exp \left\{ -i \int_{t_0} ds \frac{[\mathbf{p} + \mathbf{A}(s)]^2}{2} + i \frac{\kappa^2}{2} \tilde{t}_0 \right\}. \quad (11)$$

B. Coulomb potential

Now, with our operational approach we derive the strong-field ionization amplitude in the case of the atomic Coulomb potential. In this case, the bound state as well as the continuum state in the eikonal approximation obtain exponential corrections proportional to $v = Z/\kappa$, with the charge Z of the atomic core. The bound state in the Coulomb potential in $r \rightarrow \infty$ asymptotics reads

$$\begin{aligned} \phi(\mathbf{r}, t) &= \phi^{(0)}(\mathbf{r}, t) \phi^{(1)}(\mathbf{r}), \\ \phi^{(1)}(\mathbf{r}) &= C \exp[v \ln(\kappa r)], \end{aligned} \quad (12)$$

where C is the normalization constant (for hydrogen-like ions with $Z = \kappa$, it is $C = \sqrt{2}$) and the continuum state in the eikonal approximation is

$$\begin{aligned} \psi(\mathbf{r}, t) &= \psi^{(0)}(\mathbf{r}, t) \psi^{(1)}(\mathbf{r}, t), \\ \psi^{(1)}(\mathbf{r}, t) &= \exp \left[i v \int_t ds \frac{\kappa}{|\mathbf{r} + \mathbf{p}(s-t) + \boldsymbol{\alpha}(s) - \boldsymbol{\alpha}(t)|} \right], \end{aligned} \quad (13)$$

where $\boldsymbol{\alpha}(t) = \int dt \mathbf{A}(t)$. The t dependence in the Coulomb correction (CC) terms is weak and can be neglected with an accuracy of ω/I_p . In this case the CC momentum amplitude of Eq. (9) reads (cf. [85])

$$m_{\mathbf{p}}^{(1)} = -i \int d^3\mathbf{r} \mathcal{M}^{(0)}(\mathbf{r}) C \exp \left\{ v \left[\ln(\kappa r) + i \int_{t_s} ds \frac{\kappa}{|\mathbf{r} + \mathbf{p}(s-t_s) + \boldsymbol{\alpha}(s) - \boldsymbol{\alpha}(t_s)|} \right] \right\}. \quad (14)$$

The s integral in the phase of Eq. (14) is diverging at the low limit $t = t_s$ at the Coulomb center $\mathbf{r} = 0$. However, the diverging term can be canceled with the bound CC term $\phi^{(1)}(\mathbf{r})$ when using appropriate approximations. We separate the diverging term in the integral of Eq. (14) $\int_{t_s} = \int_{t_s}^{t_0-i\delta} + \int_{t_0-i\delta}$, and show that with appropriate choice of the parameter δ , the diverging term $\int_{t_s}^{t_0-i\delta}$ will be canceled by the bound CC

TABLE I. Estimation of the variables and parameters via SFA for the approximate calculation of the integral in Eq. (15), where $\mathbf{r} = (r_k, r_E, r_B)$; $\mathbf{p} = (p_k, p_E, p_B)$; the components of the vectors are defined along the laser propagation direction, the laser electric field, and along the laser magnetic field; and the function $g(I_p/c^2)$ depends on I_p/c^2 .

Quantity	Nonrelativistic estimate	Relativistic estimate
r_k	0	0
r_E	$\sqrt{E_a/E_0}/\kappa$	$g(I_p/c^2)\sqrt{E_a/E_0}/\kappa$
r_B	0	0
p_{k0}	0	$c(\lambda^2 - 1)/(2\lambda)$
p_{E0}	0	0
p_{B0}	0	0
Δp_k	$\sqrt{E_0/E_a}\kappa$	$g(I_p/c^2)\sqrt{E_0/E_a}\kappa$
Δp_E	$\sqrt{E_0/E_a}E_0/\omega$	$g(I_p/c^2)\sqrt{E_0/E_a}E_0/\omega$
Δp_B	$\sqrt{E_0/E_a}\kappa$	$g(I_p/c^2)\sqrt{E_0/E_a}\kappa$

term when using the following approximations. Firstly, in the analytical calculation of CC in the continuum state, we neglect all higher-order corrections with respect to $\sqrt{E_0/E_a}$, in the spirit of ARM [85]. To apply the given approximation, we estimate the variables in the integrand of Eq. (14), with the result summarized in Table I. We refer to Ref. [83]

$$\begin{aligned} \exp \left[i\nu \int_{t_s}^{t_0-i\delta} ds \frac{\kappa}{|\mathbf{r} + \mathbf{p}(s-t_s) + \boldsymbol{\alpha}(s) - \boldsymbol{\alpha}(t_s)|} \right] &\approx \exp \left[\nu \int_0^1 d\sigma \left(\frac{\sqrt{E_0/E_a} [2\delta\kappa^2 - (\sigma-1)^2 R_E^2]}{2(\sigma-1)^2 R_E} + \frac{1}{\sigma-1} \right) \right] \\ &+ \mathcal{O}(\sqrt{E_0/E_a}) \approx [\delta\kappa^2(1/R_E - \sqrt{E_0/E_a})\sqrt{E_0/E_a}]^\nu + \mathcal{O}(\sqrt{E_0/E_a}) \\ &\approx (\delta\kappa/r_E)^\nu + \mathcal{O}(\sqrt{E_0/E_a}). \end{aligned} \quad (15)$$

The singular term at $r \rightarrow 0$ in Eq. (15) will be canceled with the similar term in the Coulomb correction of the bound state, see Eq. (14), if we choose $\delta = 1/\kappa^2$. Secondly, we approximate

$$\begin{aligned} &|\mathbf{r} + \mathbf{p}(s-t_s) + \boldsymbol{\alpha}(s) - \boldsymbol{\alpha}(t_s)| \\ &\approx |\mathbf{p}_{\max}(s-t_0) + \boldsymbol{\alpha}(s) - \boldsymbol{\alpha}(t_0) + \mathcal{O}(\sqrt{E_0/E_a})|, \end{aligned} \quad (16)$$

which again follows from the scaling laws given in Table I.

Consequently, we obtain that the correction terms are approximately independent of the coordinates and arrive at the momentum amplitude:

$$\begin{aligned} m_{\mathbf{p}}^{(1)} &= -iC \int d^3\mathbf{r} \mathcal{M}^{(0)}(\mathbf{r}) \\ &\times \exp \left[i \int_{t_0-\frac{i}{\kappa^2}}^{t_0} \frac{Z ds}{|\mathbf{p}_{\max}(s-t_0) + \boldsymbol{\alpha}(s) - \boldsymbol{\alpha}(t_0)|} \right]. \end{aligned} \quad (17)$$

The latter after the final coordinate integration yields

$$m_{\mathbf{p}}^{(1)} = C m_{\mathbf{p}}^{(0)} \exp \left[i \int_{t_0-\frac{i}{\kappa^2}}^{t_0} \frac{Z ds}{|\mathbf{p}_{\max}(s-t_0) + \boldsymbol{\alpha}(s) - \boldsymbol{\alpha}(t_0)|} \right]. \quad (18)$$

[below Eq. (21)] for the estimation $r_E = \sqrt{E_a/E_0}/\kappa$, which is the scaling of the coordinate saddle point of the integrand in Eq. (9), i.e., the point where the ionizing trajectory starts; $r_k \approx r_k(t_0) = 0$ is approximated, assuming that the most probable trajectory has zero impact parameter at t_0 near the core. Further, we express $p_{k,E,B} = p_{k,E,B0} + \Delta p_{k,E,B}$, with the most probable value of the momentum $p_{k,E,B0}$ [in the nonrelativistic theory $p_{k,E,B0} = 0$, and in the relativistic one $p_{k0} = c(\lambda^2 - 1)/(2\lambda)$, $p_{E,B0} = 0$, see Eq. (28) below], and the new variables $\Delta p_{k,E,B}$ corresponding to the momentum width of the tunneling wave packet. The latter are estimated as $\Delta p_E \sim \sqrt{E_0/E_a}E_0/\omega$, $\Delta p_k = \Delta p_B \sim \sqrt{E_0/E_a}\kappa$ according to the PPT theory [60]. In the relativistic estimations an additional factor depending on I_p/c^2 arises. Here, $\mathbf{r} = (r_k, r_E, r_B)$, $\mathbf{p} = (p_k, p_E, p_B)$, and the components of the vectors are defined along the laser propagation direction $r_k \equiv \mathbf{r} \cdot \mathbf{k}/k$, $p_k \equiv \mathbf{p} \cdot \mathbf{k}/k$, along the laser electric field $r_E \equiv -\mathbf{r} \cdot \mathbf{E}/E_0$, $p_E \equiv -\mathbf{p} \cdot \mathbf{E}/E_0$, and along the laser magnetic field $r_B \equiv -\mathbf{r} \cdot \mathbf{B}/B_0$, $p_B \equiv -\mathbf{p} \cdot \mathbf{B}/B_0$. We introduce dimensionless variables R_E, P_k, P_E, P_B , dividing the given variable over its estimated value in Table I: $R_E \equiv r_E\kappa(\sqrt{E_0/E_a})$, $P_k \equiv \Delta p_k/(\sqrt{E_0/E_a}\kappa)$, $P_E \equiv \Delta p_E/(\sqrt{E_0/E_a}E_0/\omega)$, $P_B \equiv \Delta p_B/(\sqrt{E_0/E_a}\kappa)$. Further, we apply a variable transformation $s = t_s + \sigma(t_0 - i\delta - t_s)$ and expand the integrand up to leading order in E_0/E_a in a quasistatic approximation, arriving at

III. RELATIVISTIC THEORY

In the relativistic regime we employ SFA based on the Dirac equation [92]. The ionization SFA amplitude is again formally given by Eq. (1), where the interaction Hamiltonian in the Göppert-Mayer gauge within the dressed partition [92] reads

$$H_i(\mathbf{r}, t) = \mathbf{r} \cdot \mathbf{E}(\eta), \quad (19)$$

$$H_0 = H_a - \mathbf{r} \cdot \mathbf{E}(\eta)\alpha_k, \quad (20)$$

where $\alpha_k \equiv \boldsymbol{\alpha} \cdot \hat{\mathbf{k}}$, $\boldsymbol{\alpha}$ are Dirac matrices, $\hat{\mathbf{k}}$ is the unit vector along the laser propagation direction, and $\eta = t - \hat{\mathbf{k}} \cdot \mathbf{r}/c$. The spin quantization axis is chosen along the laser magnetic field. We employ the four-vector potential of the laser field in the Göppert-Mayer gauge: $A^\mu = -[\hat{\mathbf{k}}(\mathbf{r} \cdot \mathbf{E}(\eta)), \mathbf{r} \cdot \mathbf{E}(\eta)]$. In Ref. [92] we have shown that the relativistic SFA provides more close expressions to the relativistic PPT theory [66] for the total ionization rate if the dressed partition is applied. In the dressed partition, the unperturbed bound state is corrected [92] by a factor

$$S = \exp \left(i \frac{A}{2c - I_p/c} \right). \quad (21)$$

A. Short-range potential

In the case of a short-range potential the outgoing state is the relativistic Volkov state $\psi_{\mathbf{p}}(\mathbf{r}, t) \rightarrow \psi_{\mathbf{p}}^{(0)}(\mathbf{r}, t)$:

$$\begin{aligned} \psi_{\mathbf{p}}^{(0)}(\mathbf{r}, t) = & \left(1 + \frac{(1 + \alpha_k)\boldsymbol{\alpha} \cdot \mathbf{A}(\eta)}{2c\tilde{\Lambda}}\right) \frac{cu_f}{\sqrt{(2\pi)^3\tilde{\varepsilon}}} \\ & \times \exp \left[i(\mathbf{p} + \mathbf{A}(\eta)) \cdot \mathbf{r} - i\tilde{\varepsilon}t \right. \\ & \left. + i \int_{\eta} ds \left(\frac{\mathbf{p} \cdot \mathbf{A}(s) + A(s)^2/2}{\tilde{\Lambda}} \right) \right], \quad (22) \end{aligned}$$

with the asymptotic energy $\tilde{\varepsilon} = \sqrt{c^4 + c^2\mathbf{p}^2}$, the constant of motion $\tilde{\Lambda} = \tilde{\varepsilon}/c^2 - p_k/c$, and the bispinor

$$u_f = \left(\sqrt{\frac{c^2 + \tilde{\varepsilon}}{2c^2}} \chi_f, \frac{\boldsymbol{\sigma} \cdot \mathbf{p}}{\sqrt{2(c^2 + \tilde{\varepsilon})}} \chi_f \right)^T, \quad (23)$$

where $\chi_+ = (1, 0)^T$ and $\chi_- = (0, 1)^T$. The bound state of the short-range potential is

$$\phi^{(0)}(\mathbf{r}, t) = \sqrt{\frac{\kappa}{2\pi r^2}} \exp[-\kappa r + i(I_p - c^2)t] v_i, \quad (24)$$

with the atomic momentum $\kappa = \sqrt{2I_p(1 - \frac{I_p}{2c^2})}$, and the bispinor

$$v_i = \left(\chi_i, i \frac{c(\kappa r + 1)\boldsymbol{\sigma} \cdot \mathbf{r}}{(2c^2 - I_p)r^2} \chi_i \right)^T. \quad (25)$$

We consider two cases: firstly, when there is no spin flip, $\chi_f = \chi_i = \chi_+$, and secondly, when there is a spin flip during ionization, i.e., $\chi_f = \chi_-$ and $\chi_i = \chi_+$. In the first case we have

$$\begin{aligned} m_{\mathbf{p}^+}^{(0)} = & -\frac{i(2I_p)^{1/4}}{4\pi^2} \int d^3\mathbf{r} d\eta \mathcal{S}(\eta) \mathcal{P}_+ \frac{\mathbf{r} \cdot \mathbf{E}(\eta)}{r} \exp \left\{ -i \left[\mathbf{p}_{\max} + \mathbf{A}(\eta) + \frac{c^2 - I_p - \varepsilon}{c} \hat{\mathbf{k}} \right] \cdot \mathbf{r} - i \int_{\eta} ds \left[\tilde{\varepsilon} + \frac{\mathbf{p} \cdot \mathbf{A}(s) + A(s)^2/2}{\tilde{\Lambda}} \right] \right. \\ & \left. + i(I_p - c^2)\eta - \kappa r \right\}, \quad (26) \end{aligned}$$

with

$$\begin{aligned} \mathcal{P}_+ = & \frac{2c\Lambda[-c\sqrt{I_p(2c^2 - I_p)}p_{k0} - c^2(-2\varepsilon + I_p) + 2c^4 - I_p\varepsilon] + \sqrt{2\Lambda(\varepsilon - c^2 + I_p)}[\sqrt{-I_p(-2c^2 + I_p)} + 2c^2 - I_p][\varepsilon + c(c + p_{k0})]}{2c^{3/2}\Lambda(4c^2 - 2I_p)^{3/4}\sqrt{\varepsilon(c^2 + \varepsilon)}} \\ & + O(\sqrt{E_0/E_a}), \quad (27) \end{aligned}$$

where the amplitude is evaluated at the most probable quasiclassical momentum $\mathbf{p}_{\max} = (p_{k0}, 0, 0)$, with

$$p_{k0} = c(\lambda^2 - 1)/(2\lambda), \quad (28)$$

$\lambda = (\sqrt{\varepsilon^2 + 8} - \varepsilon)/2$, $\varepsilon = 1 - I_p/c^2$ and the notations $\Lambda \equiv \tilde{\Lambda}(\mathbf{p}_{\max})$ and $\varepsilon \equiv \tilde{\varepsilon}(\mathbf{p}_{\max})$. In the second case the amplitude reads

$$\begin{aligned} m_{\mathbf{p}^-}^{(0)} = & -\frac{i(2I_p)^{1/4}}{4\pi^2} \int d^3\mathbf{r} d\eta \mathcal{S}(\eta) \mathcal{P}_- \frac{\mathbf{r} \cdot \mathbf{E}(\eta)}{r} \exp \left\{ -i \left[\mathbf{p}_{\max} + \mathbf{A}(\eta) + \frac{c^2 - I_p - \varepsilon}{c} \hat{\mathbf{k}} \right] \cdot \mathbf{r} - i \int_{\eta} ds \left[\tilde{\varepsilon} + \frac{\mathbf{p} \cdot \mathbf{A}(s) + A(s)^2/2}{\tilde{\Lambda}} \right] \right. \\ & \left. + i(I_p - c^2)\eta - \kappa r \right\}, \quad (29) \end{aligned}$$

with $\mathcal{P}_- = 0 + O(\sqrt{E_0/E_a})$. We have expanded the expressions in the parameter E_0/E_a with the relativistic atomic field $E_a = \kappa^3$ and κ along the lines of SFA. From the expansion it follows that in leading order in this parameter no spin flip occurs and, consequently, we focus only on the spin flip free process.

In the next step we approximate the η integration via SPA. Here, the η -saddle-point equation is

$$\tilde{\varepsilon} + \frac{\mathbf{p} \cdot \mathbf{A}(\eta) + A(\eta)^2/2}{\tilde{\Lambda}} + I_p - c^2 + \mathbf{r} \cdot \mathbf{E}(\eta) = 0, \quad (30)$$

which is solved perturbatively with respect to the last term, yielding the solution

$$\eta_s = \tilde{\eta}_0 + \frac{\mathbf{r} \cdot \mathbf{E}(\eta_0)\Lambda}{[\mathbf{p}_{\max} + \mathbf{A}(\eta_0)] \cdot \mathbf{E}(\eta_0)}, \quad (31)$$

with the zeroth order solution $\tilde{\eta}_0$ and $\eta_0 = \tilde{\eta}_0(\mathbf{p}_{\max})$ [92]. The time dependence of the preexponential $\partial_\eta \ln[E(\eta)] \sim \omega$ is small and can be neglected. After the η -SPA, the amplitude is

$$m_{\mathbf{p}+}^{(0)} = -i \int d^3\mathbf{r} \mathcal{M}^{(0)}(\mathbf{r}) \quad (32)$$

$$\mathcal{M}^{(0)}(\mathbf{r}) = \frac{(2I_p)^{1/4}}{4\pi^2} \mathcal{S}(\eta_0) \mathcal{P}_+ \sqrt{\frac{-2i\pi\Lambda}{[\mathbf{p}_{\max} + \mathbf{A}(\eta_0)] \cdot \mathbf{E}(\eta_0)}} \frac{\mathbf{r} \cdot \mathbf{E}(\eta_0)}{r} \exp \left\{ -i \left[\mathbf{p}_{\max} + \mathbf{A}(\eta_0) + \frac{\varepsilon - c^2 + I_p}{c} \hat{\mathbf{k}} \right] \cdot \mathbf{r} \right. \\ \left. + \frac{i[\mathbf{r} \cdot \mathbf{E}(\eta_0)]^2 \Lambda}{2[\mathbf{p}_{\max} + \mathbf{A}(\eta_0)] \cdot \mathbf{E}(\eta_0)} - \kappa r - i \int_{\tilde{\eta}_0} ds \left(\tilde{\varepsilon} + \frac{\mathbf{p} \cdot \mathbf{A}(s) + A(s)^2/2}{\tilde{\Lambda}} \right) + i(I_p - c^2) \tilde{\eta}_0 \right\}, \quad (33)$$

where terms up to the next to leading order in E_0/E_a in the exponent are kept. The remaining \mathbf{r} integral is then calculated analytically in leading order in E_0/E_a ,

$$m_{\mathbf{p}}^{(0)} = \frac{i}{\sqrt{2\pi|\mathbf{E}(\eta_0)|}} \mathcal{S} \mathcal{P}_+ \mathcal{Q} \exp \left\{ -i \int_{\tilde{\eta}_0} ds \left[\tilde{\varepsilon} + \frac{\mathbf{p} \cdot \mathbf{A}(s) + A(s)^2/2}{\tilde{\Lambda}} \right] + i(I_p - c^2) \tilde{\eta}_0 \right\}. \quad (34)$$

with the prefactor

$$\mathcal{Q} = \sqrt{\frac{\varepsilon - c^2 + I_p}{I_p}} \quad (35)$$

also evaluated at the most probable quasi-classical momentum.

B. Coulomb potential

In the relativistic case the corrections to the wave functions of the order of Z/κ due to the Coulomb potential are, for the bound state,

$$\phi(\mathbf{r}, \eta) = \phi^{(0)}(\mathbf{r}, \eta) \phi^{(1)}(\mathbf{r}) \quad (36)$$

$$\phi^{(1)}(\mathbf{r}) = C \exp[v \ln(\kappa r)], \quad (37)$$

$$v = \frac{(c^2 - I_p)Z}{c^2 \sqrt{I_p(2 - I_p/c^2)}}, \quad (38)$$

with the normalization constant $C = 2^{\nu-1/2} \sqrt{\frac{\nu+1}{\Gamma(2\nu+1)}}$ for hydrogen-like systems with $Z = \kappa$, and for the continuum state,

$$\psi(\mathbf{r}, \eta) = \psi^{(0)}(\mathbf{r}, \eta) \psi^{(1)}(\mathbf{r}, \eta) \quad (39)$$

$$\psi^{(1)}(\mathbf{r}, \eta) = \exp \left\{ i \int_{\eta} ds \frac{Z\tilde{\varepsilon}(s)}{\tilde{\Lambda}c^2} \frac{1}{|\mathbf{r} + [\mathbf{p}(s - \eta) + \boldsymbol{\alpha}(s) - \boldsymbol{\alpha}(\eta)]/\tilde{\Lambda} + \mathbf{r}_k(s, \eta)|} \right\}, \quad (40)$$

with $\mathbf{r}_k(s, \eta) = \hat{\mathbf{k}}\{\mathbf{p} \cdot [\boldsymbol{\alpha}(s) - \boldsymbol{\alpha}(\eta)] + \beta(s) - \beta(\eta)\}/(c\tilde{\Lambda}^2)$, $\beta = \int ds \mathbf{A}^2/2$ and $\tilde{\varepsilon}(\eta) = \tilde{\varepsilon} + [\mathbf{p} \cdot \mathbf{A}(\eta) + A(\eta)^2/2]/\tilde{\Lambda}$.

The singularity in the s integral in the phase of Eq. (39) is removed using the same procedure as in the nonrelativistic case. The first term in the integral $\int_{\eta_s}^{\eta_0-i\delta} = \int_{\eta_s}^{\eta_0-i\delta} + \int_{\eta_0-i\delta}$ is divergent, which is canceled with the bound CC term $\phi^{(1)}(\mathbf{r})$, when using an appropriate value for the parameter δ .

Taking into account that the η dependence in the CC terms is weak, the momentum amplitude for the Coulomb potential is approximated by Eq. (32) including extra CC terms:

$$m_{\mathbf{p}+}^{(1)} = -iC \int d^3\mathbf{r} \mathcal{M}^{(0)}(\mathbf{r}) \exp \left\{ v \ln(\kappa r) + i \int_{\eta_s} ds \frac{Z\tilde{\varepsilon}(s)}{\tilde{\Lambda}c^2} \frac{1}{|\mathbf{r} + (\mathbf{p}(s - \eta_s) + \boldsymbol{\alpha}(s) - \frac{\boldsymbol{\alpha}(\eta_s)}{\tilde{\Lambda}}) + \mathbf{r}_k(s, \eta_s)|} \right\}. \quad (41)$$

The choice of δ for the singularity removal is possible when the following approximations are applied. We integrate the Coulomb correction in the continuum state analytically around η_s :

$$\exp \left[i \int_{\eta_s}^{\eta_0-i\delta} \frac{Z\tilde{\varepsilon}(s)ds}{\tilde{\Lambda}c^2 |\mathbf{r} + [\mathbf{p}(s - \eta_s) + \boldsymbol{\alpha}(s) - \boldsymbol{\alpha}(\eta_s)]/\tilde{\Lambda} + \mathbf{r}_k(s, \eta_s)|} \right] \approx \left(\frac{\sqrt{3}\lambda\kappa\delta}{\sqrt{(4 - \lambda^2)r_E}} \right)^v, \quad (42)$$

where the same method as in the derivation of Eq. (15) is applied, i.e., the same scaled variables are introduced (R_E , P_k and P_E , P_B), the variable transformation $s = \eta_s + \sigma(\eta_0 - i\delta - \eta_s)$ is used, and then, before analytical integration the integrand is expanded in $\sqrt{E_0/E_a}$ in a quasistatic approximation, using estimations of Table I. Further, the atomic correction term is in

leading order in E_0/E_a ,

$$(\kappa r)^v = \left(\kappa \frac{\sqrt{4 - \lambda^2} r_E}{\sqrt{3}} \right)^v. \quad (43)$$

With the choice $\delta = 1/(\lambda\kappa^2) = \Lambda/\kappa^2 \approx [1 - \kappa^2/(6c^2)]/\kappa^2$, we cancel the singular term of the Coulomb correction to the bound state. Then, we approximate in leading order in E_0/E_a :

$$|\mathbf{r} + [\mathbf{p}(s - \eta_s) + \boldsymbol{\alpha}(s) - \boldsymbol{\alpha}(\eta_s)]/\tilde{\Lambda} + \mathbf{r}_k(s, \eta_s)| \approx |[\mathbf{p}_{\max}(s - \eta_0) + \boldsymbol{\alpha}(s) - \boldsymbol{\alpha}(\eta_0)]/\Lambda + \mathbf{r}_k(s, \eta_0) + \mathcal{O}(\sqrt{E_0/E_a})|. \quad (44)$$

Thus, we conclude that the correction terms are approximately independent of the coordinates, and arrive at the momentum amplitude,

$$m_{\mathbf{p}}^{(1)} = -iC \int d^3\mathbf{r} \mathcal{M}^{(0)}(\mathbf{r}) \exp \left\{ i \int_{\eta_0 - i\Lambda/\kappa^2} \frac{Z\varepsilon(s)/(c^2\Lambda) ds}{|\mathbf{p}_{\max}(s - \eta_0) + \boldsymbol{\alpha}(s) - \boldsymbol{\alpha}(\eta_0) + \mathbf{r}_k(s, \eta_0)|} \right\}. \quad (45)$$

After the final coordinate integration, this yields

$$m_{\mathbf{p}}^{(1)} = C m_{\mathbf{p}}^{(0)} \exp \left\{ i \int_{\eta_0 - i\Lambda/\kappa^2} \frac{Z\varepsilon(s)/(c^2\Lambda) ds}{|\mathbf{p}_{\max}(s - \eta_0) + \boldsymbol{\alpha}(s) - \boldsymbol{\alpha}(\eta_0) + \mathbf{r}_k(s, \eta_0)|} \right\}. \quad (46)$$

Equation (46) is the main result of the paper, providing the Coulomb-corrected strong-field ionization amplitude for the relativistic regime using the ARM approach.

IV. COMPARISON WITH THE RELATIVISTIC CCSFA

Comparison of the total ionization probability in relativistic ARM (RARM) with CCSFA of Ref. [92] and PPT theories is provided in Fig. 1. The RARM probability coincides with the PPT theory, whereas the CCSFA overestimates slightly the PPT theory. Here, the rate is calculated in leading order in E_0/E_a and the final momentum integration is accomplished via SPA at the most probable momentum after a transformation from the asymptotic momentum \mathbf{p} to the tunnel exit distribution $(\eta_e, p_{e,B}, p_{e,k})$, with $p_E + A(\eta_e) = 0$, $p_B = p_{e,B}$, and $p_k = p_{k,e} + A(\eta_e)^2/2/c/\tilde{\Lambda}$.

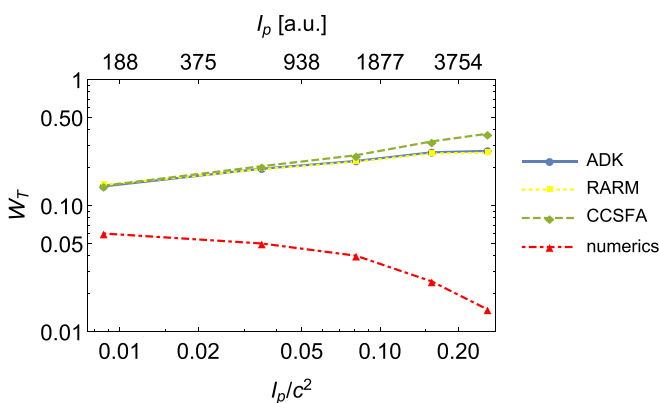


FIG. 1. Comparison of the theoretical data for the total probability W_T per the laser period with the result of the numerical calculation [104]: via RARM (yellow short-dashed line with squares) with CCSFA of Ref. [83] (green long-dashed line with diamonds) using dressed partition, ADK (blue solid line) theories at $Z/\kappa = 1$, and (red dash-dotted line with triangles) the numerical calculations via the Klein-Gordon equation [104]. Numerical calculations in Ref. [104] have been carried out for the ionization energies $I_p/c^2 = 0.00866, 0.0351, 0.0809, 0.158, 0.259$, using $E_0/E_a \approx 1/16$.

In Fig. 1, the comparison of the results for the total probability per laser cycle via RARM, CCSFA, and PPT with the numerical calculation of Hafizi *et al.* using the Klein-Gordon equation [104] is shown. While the theoretical results almost coincide with each other, there is a significant deviation from the numerical calculation, especially at high values of I_p/c^2 . There are two reasons for the deviation of the analytical quasi-classical theories, CCSFA and RARM, with respect to the numerical result. We compare the total ionization rate via RARM based on the Dirac equation with the numerical solution of the Klein-Gordon equation, intuitively assuming that for the total ionization rate spin effects would not matter much. However, this assumption is valid only for $I_p/c^2 \ll 1$. The results of Refs. [60,109] show that at large $I_p/c^2 \sim 1$ spin asymmetry arises in the ionization (difference in ionization probability of different spin states), which will lead to a modification of the spin averaged probability. However, this effect is of the order of at most 1% even for hydrogen-like uranium and cannot account for the large discrepancy apparent in Fig. 1. The main source of the deviation (by a factor of ~ 20) possibly comes from the Stark shift and polarization of the atomic state in strong fields near the threshold of the over-the-barrier ionization. These corrections are especially relevant in the near-threshold regime of tunneling ionization at $E_0/E_a \sim 1/10$, which is the case in the numerical data of Hafizi ($E_0/E_a \sim 1/16$). We assume that this deviation could be corrected, at least partly, via the next-order quasi-classical CCs to the eikonal approximation. As is shown in Ref. [82] with one-dimensional (1D) CCSFA for the nonrelativistic theory [see Eq. (47) in this reference], this kind of correction leads to a decrease of the tunneling ionization probability. High-order quasi-classical CCs within ARM are generally possible, but it would require the change of the matching procedure to the bound state and, consequently, the change of the complex shift of the time integration.

From a technical point of view, RARM has a clear advantage with respect to relativistic eikonal CCSFA of Refs. [29,92] when applying SPA. While in RARM the

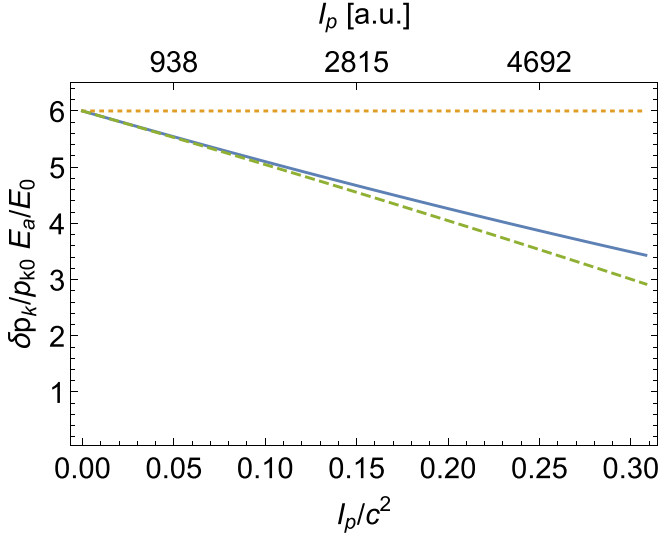


FIG. 2. The nondipole shift of the peak of the longitudinal momentum due to the subbarrier CC for hydrogen-like highly charged ions: via RARM (blue solid) via Eq. (49), via nondipole CCSFA [19] (orange short dash), and via the approximate Eq. (50) with the leading correction $\sim I_p/c^2$ (green long dash).

ionization amplitude is found via a one-dimensional η -SPA, in CCSFA at least the two-dimensional (in the case of linear polarization) or four-dimensional (in the case of elliptical polarization) SPA for (\mathbf{r}, η) integrations is required.

A disadvantage of RARM is that it includes accurately the CC near the tunnel exit, but overestimates those due to rescatterings. To account for CC at hard recollisions, the generalized eikonal approximation (GEA) has been developed on the basis of CCSFA. Generalization to elliptical polarization in both cases (RARM/CCSFA) is possible.

V. COMPARISON WITH THE NONDIPOLE CCSFA

To test the derived RARM theory, it will be useful to compare its results with those of the nondipole CCSFA describing Coulomb effects in strong-field ionization in the nondipole regime. In the nondipole CCSFA only the first relativistic correction to the dipole theory of the order of $1/c$ is included. We expect that the fully relativistic theory will coincide with the nondipole one in the limit $I_p/c^2 \ll 1$, with significant deviations at $I_p \sim c^2$, as $1/c^2$ terms are neglected in the nondipole theory.

While in the nonrelativistic theory the electron transverse momentum distribution at the tunnel exit has a peak at zero momentum, in the relativistic treatment the peak is shifted to $p_{k0} = I_p/3c$ along the laser propagation direction due to the subbarrier effect of the laser magnetic field [14]. Recently, we showed [19] within nondipole CCSFA that the subbarrier Coulomb effect increases counterintuitively the nondipole shift of the longitudinal momentum p_k at the tunnel exit:

$$p_k = p_{k0} + \delta p_k$$

$$\delta p_k = 6(E_0/E_a)p_{k0}. \quad (47)$$

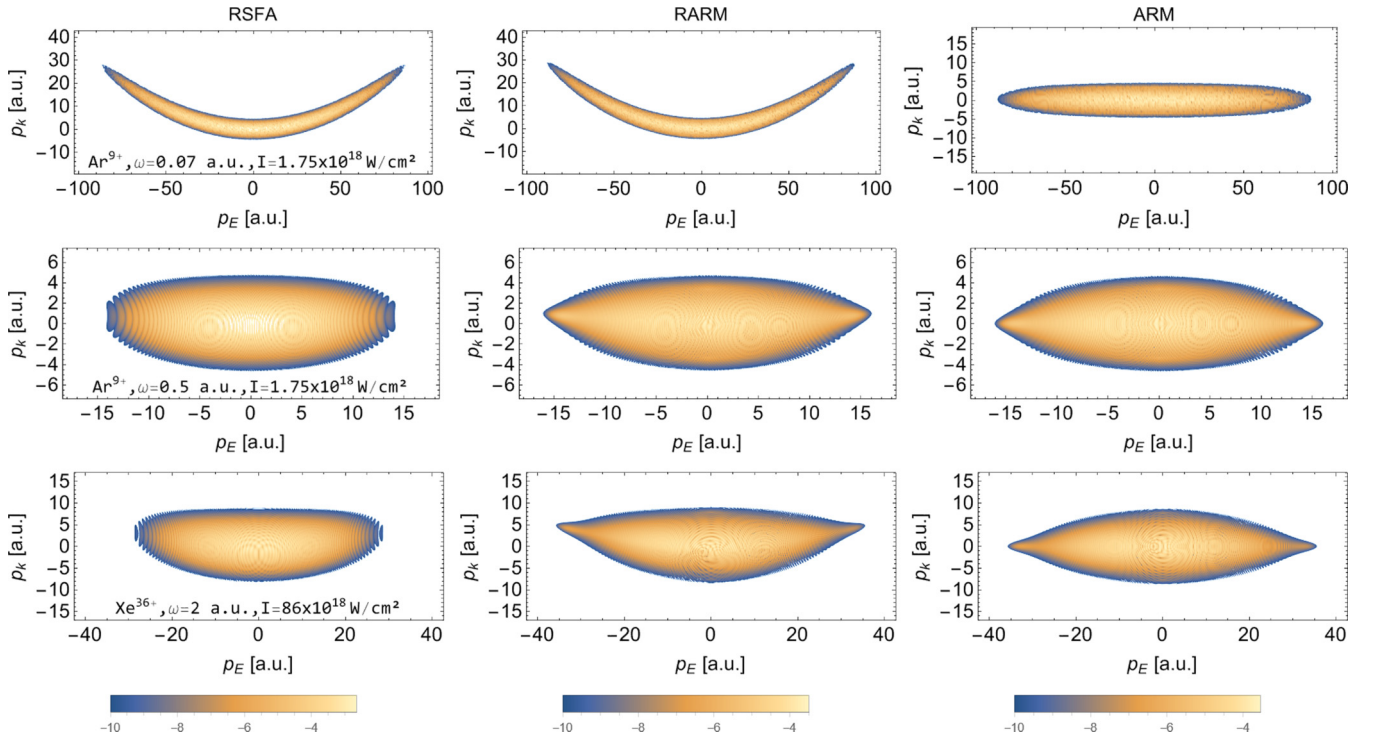


FIG. 3. PMD in the case of HECE: (first column) via relativistic plain SFA (RSFA), (second column) via RARM, (third column) via nonrelativistic ARM; (first line) for Ar^{9+} , $\nu = 2.34$, $I_p = 17.63$ atomic units (AU), laser intensity 1.75×10^{18} W/cm 2 ($E_0 = 7.07$ AU), and $\omega = 0.07$ AU ($\nu = 0.043$, $\xi = 0.74$, $Z\omega/E_0 = 0.14$); (second line) for Ar^{9+} , and XUV beam $\omega = 0.5$ AU of intensity 1.75×10^{18} W/cm 2 ($\nu = 0.043$, $\xi = 0.1$, $Z\omega/E_0 = 0.99$); (third line) for Xe^{36+} , $\nu = 2.626$, $I_p = 93.94$ AU, and X-ray beam of intensity 8.6×10^{19} W/cm 2 ($E_0 = 65.4$ AU) and $\omega = 2$ AU ($\nu = 0.1$, $\xi = 0.24$, $Z\omega/E_0 = 1.13$).

The CC effect induces an additional dependence of the longitudinal momentum shift on E_0/E_a . Let us compare the RARM result for the relativistic shift of the peak of the longitudinal momentum due to the subbarrier CC with the nondipole theory of Ref. [19], see Fig. 2, where $\delta p_k/[(E_0/E_a)p_{k0}]$ for a hydrogen-like highly charged ion is presented. According to the nondipole approximate theory [19], $\delta p_k/[(E_0/E_a)p_{k0}] = 6$ [Eq. (47)]. The relativistic shift of the peak of the longitudinal momentum presented in Fig. 2 is calculated analytically using the exact RARM theory. To this end, the atomic as well as the laser action is expanded up to the next-to-leading order with respect to E_0/E_a :

$$S_0(p_k) = S_0(p_{k0}) - \frac{2\kappa\lambda(\lambda^2 + 2)}{\sqrt{12 - 3\lambda^2(\lambda^2 + 1)^2}} \frac{(p_k - p_{k0})^2}{E_0},$$

$$S_1(p_k) = S_1(p_{k0}) + \frac{2\sqrt{-\lambda^4 + 5\lambda^2 - 4}\left(1 - \frac{\lambda^2 + \lambda - 2}{\lambda}\right)}{(\lambda^2 + 1)\kappa} \times (p - p_{k0}). \quad (48)$$

The longitudinal momentum distribution is given by $\exp\{S\} = \exp[S_0(p_k) + S_1(p_k)]$. It has a maximum at $p_k - p_{k0} = -S'_1(p_{k0})/S''_0(p_{k0})$, which, after using the expansion over $\lambda - 1 \sim I_p/c^2$, reads

$$p_k - p_{k0} = -\frac{\sqrt{3}(4 - \lambda^2)^{3/2}(\lambda^2 - 2)(\lambda^2 + 1)E_0}{\lambda^2(\lambda^2 + 2)} \frac{E_0}{\kappa^3} p_{k0} \quad (49)$$

$$\approx [6 - 28(\lambda - 1)] \frac{E_0}{\kappa^3} p_{k0} + O(\lambda - 1), \quad (50)$$

with $p_{k0} = c(\lambda^2 - 1)/2\lambda \approx I_p/3c$. Thus, the first term of the shift of the most probable momentum in the propagation direction due to the subbarrier CC corresponds to the nondipole result, and the second term $\sim \lambda - 1 = I_p/(3c^2)$ is the relativistic CC. The momentum shift coincides with the nondipole result at small $I_p/c^2 \ll 1$. It is reduced when taking into account the relativistic corrections $\sim I_p/c^2$. This is because the subbarrier CC originates from the bound state CC, as discussed in Ref. [19]. The decrease of the parameter $\nu \approx 1 - I_p/c^2$ with higher I_p/c^2 , see Eq. (38), yields a larger width of the bound state in momentum space. Then, the most probable subbarrier tunneling trajectory begins at the atomic core with larger p_k , ending up at the tunnel exit with a smaller one, because the magnetic-field-induced momentum drift along the propagation direction is fixed.

Heuristically, the momentum shift can be estimated via $S'_a(p_k) \sim \partial_{p_k} \{\ln[\kappa\sqrt{\mathbf{r}(\eta)^2}]\} \sim \partial_{p_k} \{\ln[\kappa\sqrt{\mathbf{p}_i^2(s - t_i)^2/\Lambda}]\} \sim \partial_{p_k} \{\ln(\kappa^2(s - t_i)/\Lambda)\} \sim \partial_{p_k} \{\ln(\Lambda)\} \sim \partial_{p_k} \{p_k/c\} \sim 1/c$. With $p_{k,0} \sim \kappa^2/(6c)$ and $S''_0(p_{k0}) \sim \kappa/E_0$, the momentum shift $-S'_a(p_{k0})/S''_0(p_{k0}) \sim 6E_0/\kappa^3 p_{k0}$ follows.

VI. HIGH-ENERGY COULOMB ENHANCEMENT IN THE CASE OF HCIs

We apply the relativistic ARM theory for the investigation of the Coulomb enhancement effect at the cutoff of the direct ionization channel in the relativistic domain with HCIs. This effect of the high-energy Coulomb enhancement (HECE) in the nonrelativistic regime is known, described

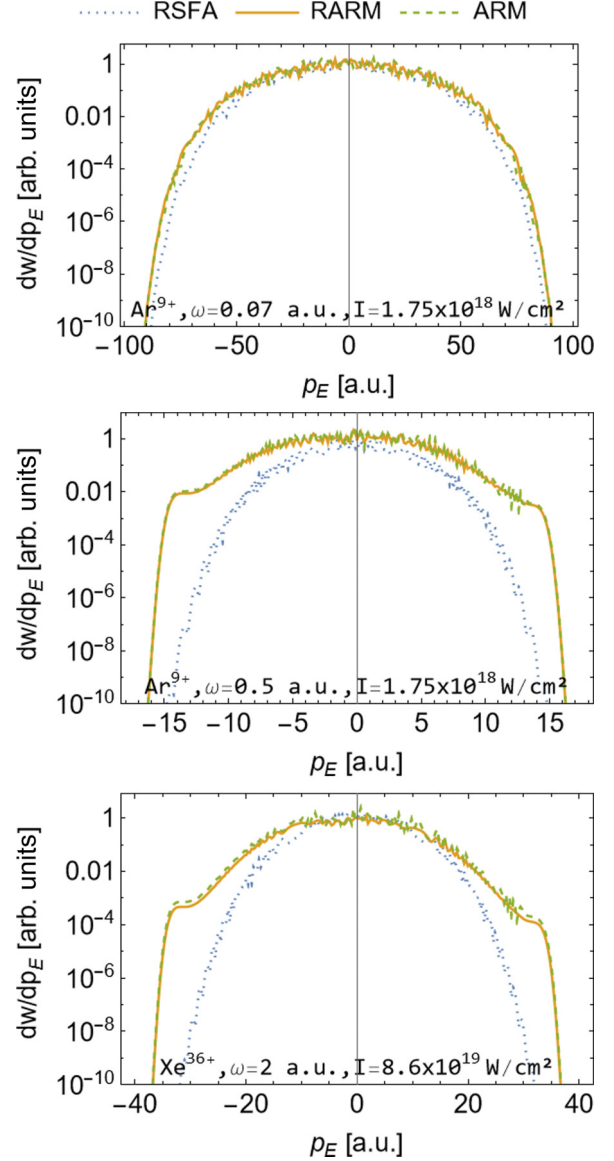


FIG. 4. The HECE spectra of Fig. 3 integrated over p_k , for the same species and the laser fields: (blue dotted) via RSFA, (orange solid) via RARM, (green dashed) via nonrelativistic ARM; (first line) for Ar^{9+} , $\nu = 2.34$, $I_p = 17.63$ AU, laser intensity 1.75×10^{18} W/cm 2 ($E_0 = 7.07$ AU), and $\omega = 0.07$ AU ($\nu = 0.043$, $\xi = 0.74$, $Z\omega/E_0 = 0.14$); (second line) for Ar^{9+} , and XUV beam $\omega = 0.5$ AU of intensity 1.75×10^{18} W/cm 2 ($\nu = 0.043$, $\xi = 0.1$, $Z\omega/E_0 = 0.99$); (third line) for Xe^{36+} , $\nu = 2.626$, $I_p = 93.94$ AU, and X-ray beam of intensity 8.6×10^{19} W/cm 2 ($E_0 = 65.4$ AU) and $\omega = 2$ AU ($\nu = 0.1$, $\xi = 0.24$, $Z\omega/E_0 = 1.13$). The distributions are rescaled to the peak value.

in Refs. [88,106]. The effect emerges due to the Coulomb momentum transfer in the continuum. The electron trajectory that ends up at the cutoff of the direct channel starts at the tunnel exit at relatively weak fields and stays near the exit a long time, obtaining rather large Coulomb momentum transfer [106]. The parameter which quantifies HECE is $Z\omega/E_0$ [88]. In the calculation of the continuum CC, the continuum action is expanded in E_0/E_a , which yields an expansion in the

imaginary part of the complex trajectory:

$$S_1[\mathbf{r}(\eta)] = S_1\{\text{Re}[\mathbf{r}(\eta)]\} + i\text{Im}[\mathbf{r}(\eta)] \cdot \nabla S_1\{\text{Re}[\mathbf{r}(\eta)]\}. \quad (51)$$

We calculated PMD for three cases via Eq. (46), presented in Fig. 3. In the first case we consider HECE for Ar^{9+} $I_p = 479.76$ eV, $Z_{\text{eff}} = 14.008$, $\nu = 2.34$, laser intensity 1.75×10^{18} W/cm² ($E_0 = 7.07$ AU) using IR laser beam with $\omega = 0.07$ AU ($\nu = 0.043$, $\xi = 0.74$, $Z\omega/E_0 = 0.14$). In the second case the same atomic species are used with an XUV (extreme ultra-violet) laser beam ($\omega = 0.5$ AU) of the same high intensity 1.75×10^{18} W/cm² ($\nu = 0.043$, $\xi = 0.1$, $Z\omega/E_0 = 0.99$). And in the third example we consider Xe^{36+} ($I_p = 2556$ eV, $\nu = 2.626$) exposed to the strong X-ray field ($\omega = 2$ AU) $E_0 = 65.4$ AU ($\nu = 0.1$, $\xi = 0.24$, $Z\omega/E_0 = 1.13$). To elucidate the HECE effect we compare PMD via RARM with the plain relativistic SFA. The transverse width of PMD is $p_B = \sqrt{E_0/\kappa}/2$.

In the first example, the continuum relativistic parameter ξ is the largest. Consequently, we see the parabolic dependence of p_k with respect to p_E , which is typical for the electron relativistic dynamics in the continuum, and absent in the non-relativistic consideration (third column in Fig. 3). However, the Coulomb enhancement (HECE) parameter $Z\omega/E_0$ is the smallest in the first example, and we do not see a significant Coulomb effect, HECE, as the integrated spectrum over p_k coincides with the plain SFA result. The HECE parameter increases for the second and the third cases, which results in the appearance of significant shoulders in PMD at $2U_p$ energies. The continuum relativistic features in PMD also enhance. The relativistic and nonrelativistic PMD via ARM are clearly distinguishable (second and third columns) by the parabolic feature in p_k dependence of p_E ; however, after p_k

integration the HECE features are the same (Fig. 4). The bound state relativistic character is not very pronounced in the given examples as $\nu < 0.1$.

VII. CONCLUSION

We have generalized the ARM theory for the relativistic regime of strong-field ionization. The CCSFA based on the eikonal wave function for the continuum electron (accounting for the Coulomb interaction of the outgoing electron with the atomic core) has a singularity in the eikonal phase at the Coulomb center, where strong-field ionization starts in the imaginary time. While in the PPT theory the singularity is remedied via matching the continuum wave function to the undisturbed bound state one, in the ARM theory this procedure is equivalent to the shift of the starting point of the time integration in the ionization amplitude by an appropriate imaginary value. In this paper we have found how the value of the corresponding imaginary time shift is modified in the relativistic regime, which eliminates the singularity of the relativistic CCSFA amplitude for ionization.

The advantage of RARM with respect to CCSFA is that it simplifies the calculations of the ionization amplitude using SPA. However, CCSFA offers a possibility for systematic second-order Coulomb corrections when using SPA in the coordinate integration, rather than the matching procedure with the bound state. Moreover, CCSFA allows for the development of the generalized eikonal approximation to treat CC at hard recollisions. For subbarrier CC, the RARM provides results similar to the nondipole CCSFA.

Finally, we employed RARM theory to calculate the Coulomb enhancement of the above-threshold ionization yield at the cutoff of the directly ionized electrons in the relativistic regime.

-
- [1] J. Ullrich, R. Moshhammer, A. Dorn, R. Dörner, L. P. H. Schmidt, and H. Schmidt-Böcking, Recoil-ion and electron momentum spectroscopy: Reaction-microscopes, *Rep. Prog. Phys.* **66**, 1463 (2003).
 - [2] M. Weger, J. Maurer, A. Ludwig, L. Gallmann, and U. Keller, Transferring the attoclock technique to velocity map imaging, *Opt. Express* **21**, 21981 (2013).
 - [3] C. T. L. Smeenk, L. Arissian, B. Zhou, A. Mysyrowicz, D. M. Villeneuve, A. Staudte, and P. B. Corkum, Partitioning of the Linear Photon Momentum in Multiphoton Ionization, *Phys. Rev. Lett.* **106**, 193002 (2011).
 - [4] A. Ludwig, J. Maurer, B. W. Mayer, C. R. Phillips, L. Gallmann, and U. Keller, Breakdown of the Dipole Approximation in Strong-Field Ionization, *Phys. Rev. Lett.* **113**, 243001 (2014).
 - [5] J. Maurer, B. Willenberg, J. Daněk, B. W. Mayer, C. R. Phillips, L. Gallmann, M. Klaiber, K. Z. Hatsagortsyan, C. H. Keitel, and U. Keller, Probing the ionization wave packet and recollision dynamics with an elliptically polarized strong laser field in the nondipole regime, *Phys. Rev. A* **97**, 013404 (2018).
 - [6] B. Willenberg, J. Maurer, B. W. Mayer, and U. Keller, Sub-cycle time resolution of multi-photon momentum transfer in strong-field ionization, *Nat. Commun.* **10**, 5548 (2019).
 - [7] A. Hartung, S. Eckart, S. Brennecke, J. Rist, D. Trabert, K. Fehre, M. Richter, H. Sann, S. Zeller, K. Henrichs *et al.*, Magnetic fields alter strong-field ionization, *Nat. Phys.* **15**, 1222 (2019).
 - [8] N. Haram, I. Ivanov, H. Xu, K. T. Kim, A. Atia-tul-Noor, U. S. Sainadh, R. D. Glover, D. Chetty, I. V. Litvinyuk, and R. T. Sang, Relativistic Nondipole Effects in Strong-Field Atomic Ionization at Moderate Intensities, *Phys. Rev. Lett.* **123**, 093201 (2019).
 - [9] N. Haram, R. T. Sang, and I. V. Litvinyuk, Transverse electron momentum distributions in strong-field ionization: Nondipole and Coulomb focusing effects, *J. Phys. B: At. Mol. Opt. Phys.* **53**, 154005 (2020).
 - [10] A. Hartung, S. Brennecke, K. Lin, D. Trabert, K. Fehre, J. Rist, M. S. Schöffler, T. Jahnke, L. P. H. Schmidt, M. Kunitski, M. Lein, R. Dörner, and S. Eckart, Electric Nondipole Effect in Strong-Field Ionization, *Phys. Rev. Lett.* **126**, 053202 (2021).
 - [11] K. Lin, S. Brennecke, H. Ni, X. Chen, A. Hartung, D. Trabert, K. Fehre, J. Rist, X.-M. Tong, J. Burgdörfer, L. P. H. Schmidt, M. S. Schöffler, T. Jahnke, M. Kunitski, F. He, M. Lein, S. Eckart, and R. Dörner, Magnetic-Field Effect in High-Order Above-Threshold Ionization, *Phys. Rev. Lett.* **128**, 023201 (2022).

- [12] K. Lin, X. Chen, S. Eckart, H. Jiang, A. Hartung, D. Trabert, K. Fehre, J. Rist, L. P. H. Schmidt, M. S. Schöffler, T. Jahnke, M. Kunitski, F. He, and R. Dörner, Magnetic-Field Effect as a Tool to Investigate Electron Correlation in Strong-Field Ionization, *Phys. Rev. Lett.* **128**, 113201 (2022).
- [13] K. Lin, S. Eckart, A. Hartung, D. Trabert, K. Fehre, J. Rist, L. P. H. Schmidt, M. S. Schöffler, T. Jahnke, M. Kunitski, and R. Dörner, Photoelectron energy peaks shift against the radiation pressure in strong field ionization, *Sci. Adv.* **8**, eabn7386 (2022).
- [14] M. Klaiber, E. Yakaboylu, H. Bauke, K. Z. Hatsagortsyan, and C. H. Keitel, Under-the-Barrier Dynamics in Laser-Induced Relativistic Tunneling, *Phys. Rev. Lett.* **110**, 153004 (2013).
- [15] S. Chelkowski, A. D. Bandrauk, and P. B. Corkum, Photon Momentum Sharing between an Electron and an Ion in Photoionization: From One-Photon (Photoelectric Effect) to Multiphoton Absorption, *Phys. Rev. Lett.* **113**, 263005 (2014).
- [16] D. Cricchio, E. Fiordilino, and K. Z. Hatsagortsyan, Momentum partition between constituents of exotic atoms during laser-induced tunneling ionization, *Phys. Rev. A* **92**, 023408 (2015).
- [17] S. Chelkowski, A. D. Bandrauk, and P. B. Corkum, Photon-momentum transfer in multiphoton ionization and in time-resolved holography with photoelectrons, *Phys. Rev. A* **92**, 051401(R) (2015).
- [18] P.-L. He, D. Lao, and F. He, Strong Field Theories beyond Dipole Approximations in Nonrelativistic Regimes, *Phys. Rev. Lett.* **118**, 163203 (2017).
- [19] P.-L. He, M. Klaiber, K. Z. Hatsagortsyan, and C. H. Keitel, Nondipole Coulomb sub-barrier ionization dynamics and photon momentum sharing, *Phys. Rev. A* **105**, L031102 (2022).
- [20] M. Førre, J. P. Hansen, L. Kocbach, S. Selstø, and L. B. Madsen, Nondipole Ionization Dynamics of Atoms in Superintense High-Frequency Attosecond Pulses, *Phys. Rev. Lett.* **97**, 043601 (2006).
- [21] T. Keil and D. Bauer, Coulomb-corrected strong-field quantum trajectories beyond dipole approximation, *J. Phys. B: At. Mol. Opt. Phys.* **50**, 194002 (2017).
- [22] J. F. Tao, Q. Z. Xia, J. Cai, L. B. Fu, and J. Liu, Coulomb rescattering in nondipole interaction of atoms with intense laser fields, *Phys. Rev. A* **95**, 011402(R) (2017).
- [23] J. Daněk, M. Klaiber, K. Z. Hatsagortsyan, C. H. Keitel, B. Willenberg, J. Maurer, B. W. Mayer, C. R. Phillips, L. Gallmann, and U. Keller, Interplay between Coulomb-focusing and non-dipole effects in strong-field ionization with elliptical polarization, *J. Phys. B: At. Mol. Opt. Phys.* **51**, 114001 (2018).
- [24] J. Daněk, K. Z. Hatsagortsyan, and C. H. Keitel, Analytical approach to Coulomb focusing in strong-field ionization. I. Nondipole effects, *Phys. Rev. A* **97**, 063409 (2018).
- [25] J. Daněk, K. Z. Hatsagortsyan, and C. H. Keitel, Analytical approach to Coulomb focusing in strong-field ionization. II. Multiple recollisions, *Phys. Rev. A* **97**, 063410 (2018).
- [26] B. Willenberg, J. Maurer, U. Keller, J. Daněk, M. Klaiber, N. Teeny, K. Z. Hatsagortsyan, and C. H. Keitel, Holographic interferences in strong-field ionization beyond the dipole approximation: The influence of the peak and focal-volume-averaged laser intensities, *Phys. Rev. A* **100**, 033417 (2019).
- [27] M. Klaiber, K. Z. Hatsagortsyan, and C. H. Keitel, Above-threshold ionization beyond the dipole approximation, *Phys. Rev. A* **71**, 033408 (2005).
- [28] P.-L. He, K. Z. Hatsagortsyan, and C. H. Keitel, Nondipole Time Delay and Double-Slit Interference in Tunneling Ionization, *Phys. Rev. Lett.* **128**, 183201 (2022).
- [29] M. Klaiber, K. Z. Hatsagortsyan, and C. H. Keitel, Subcycle time-resolved nondipole dynamics in tunneling ionization, *Phys. Rev. A* **105**, 053107 (2022).
- [30] H. Ni, S. Brennecke, X. Gao, P.-L. He, S. Donsa, I. Březinová, F. He, J. Wu, M. Lein, X.-M. Tong, and J. Burgdörfer, Theory of Subcycle Linear Momentum Transfer in Strong-Field Tunneling Ionization, *Phys. Rev. Lett.* **125**, 073202 (2020).
- [31] D. Habibović and D. B. Milošević, Strong-field ionization of atoms beyond the dipole approximation, *Phys. Rev. A* **106**, 033101 (2022).
- [32] M. M. Lund and L. B. Madsen, Nondipole photoelectron momentum shifts in strong-field ionization with mid-infrared laser pulses of long duration, *J. Phys. B: At. Mol. Opt. Phys.* **54**, 165602 (2021).
- [33] B. Böning and S. Fritzsche, Above-threshold ionization driven by Gaussian laser beams: Beyond the electric dipole approximation, *J. Phys. B: At. Mol. Opt. Phys.* **54**, 144002 (2021).
- [34] L. B. Madsen, Nondipole effects in tunneling ionization by intense laser pulses, *Phys. Rev. A* **105**, 043107 (2022).
- [35] S. Fritzsche and B. Böning, Lorentz-force shifts in strong-field ionization with mid-infrared laser fields, *Phys. Rev. Res.* **4**, 033031 (2022).
- [36] R. Kahvedžić and S. Gräfe, Strong-field approximation with leading-order nondipole corrections, *Phys. Rev. A* **105**, 063102 (2022).
- [37] X. Mao, H. Ni, X. Gong, J. Burgdörfer, and J. Wu, Subcycle resolved strong-field tunneling ionization: Identification of magnetic dipole and electric quadrupole effects, *Phys. Rev. A* **106**, 063105 (2022).
- [38] S. Brennecke and M. Lein, High-order above-threshold ionization beyond the electric dipole approximation: Dependence on the atomic and molecular structure, *Phys. Rev. A* **98**, 063414 (2018).
- [39] S. Brennecke and M. Lein, Nondipole modification of the ac stark effect in above-threshold ionization, *Phys. Rev. A* **104**, L021104 (2021).
- [40] M. Klaiber, K. Z. Hatsagortsyan, J. Wu, S. S. Luo, P. Grugan, and B. C. Walker, Limits of Strong Field Rescattering in the Relativistic Regime, *Phys. Rev. Lett.* **118**, 093001 (2017).
- [41] E. Jones, Z. Germain, J. Niessner, D. Milliken, J. Scilla, L. Kelley, J. MacDonald, and B. C. Walker, Radiation for laser-driven rescattering near the ultimate high-energy cutoff: The single-atom response and bremsstrahlung limit, *Phys. Rev. A* **103**, 023113 (2021).
- [42] L. Kelley, Z. Germain, E. C. Jones, D. Milliken, and B. C. Walker, Inner shell excitation by strong field laser rescattering: Optimal laser conditions for high energy recollision, *J. Opt. Soc. Am. B* **38**, 3646 (2021).
- [43] J. W. Yoon, Y. G. Kim, I. W. Choi, J. H. Sung, H. W. Lee, S. K. Lee, C. H. Nam, J. H. Sung, H. W. Lee, S. K. Lee, S. K. Lee, S. K. Lee, C. H. Nam, C. H. Nam, and C. H. Nam, Realization of laser intensity over 10^{23} W/cm², *Optica* **8**, 630 (2021).

- [44] C. I. Moore, A. Ting, S. J. McNaught, J. Qiu, H. R. Burris, and P. Sprangle, A Laser-Accelerator Injector Based on Laser Ionization and Ponderomotive Acceleration of Electrons, *Phys. Rev. Lett.* **82**, 1688 (1999).
- [45] E. A. Chowdhury, C. P. J. Barty, and B. C. Walker, “Non-relativistic” ionization of the *L*-shell states in argon by a “relativistic” 10^{19} W/cm² laser field, *Phys. Rev. A* **63**, 042712 (2001).
- [46] M. Dammasch, M. Dörr, U. Eichmann, E. Lenz, and W. Sandner, Relativistic laser-field-drift suppression of nonsequential multiple ionization, *Phys. Rev. A* **64**, 061402(R) (2001).
- [47] K. Yamakawa, Y. Akahane, Y. Fukuda, M. Aoyama, N. Inoue, and H. Ueda, Ionization of many-electron atoms by ultrafast laser pulses with peak intensities greater than 10^{19} W/cm², *Phys. Rev. A* **68**, 065403 (2003).
- [48] A. Maltsev and T. Ditmire, Above Threshold Ionization in Tightly Focused, Strongly Relativistic Laser Fields, *Phys. Rev. Lett.* **90**, 053002 (2003).
- [49] E. Gubbini, U. Eichmann, M. Kalashnikov, and W. Sandner, Core Relaxation in Atomic Ultrastrong Laser Field Ionization, *Phys. Rev. Lett.* **94**, 053602 (2005).
- [50] A. D. DiChiara, I. Ghebregziabher, R. Sauer, J. Waesche, S. Palaniyappan, B. L. Wen, and B. C. Walker, Relativistic MeV Photoelectrons from the Single Atom Response of Argon to a 10^{19} W/cm² Laser Field, *Phys. Rev. Lett.* **101**, 173002 (2008).
- [51] S. Palaniyappan, R. Mitchell, R. Sauer, I. Ghebregziabher, S. L. White, M. F. Decamp, and B. C. Walker, Ionization of Methane in Strong and Ultrastrong Relativistic Fields, *Phys. Rev. Lett.* **100**, 183001 (2008).
- [52] A. D. DiChiara, I. Ghebregziabher, J. M. Waesche, T. Stanev, N. Ekanayake, L. R. Barclay, S. J. Wells, A. Watts, M. Videtto, C. A. Mancuso, and B. C. Walker, Photoionization by an ultraintense laser field: Response of atomic xenon, *Phys. Rev. A* **81**, 043417 (2010).
- [53] N. Ekanayake, S. Luo, P. D. Grugan, W. B. Crosby, A. D. Camilo, C. V. McCowan, R. Scalzi, A. Tramontozzi, L. E. Howard, S. J. Wells, C. Mancuso, T. Stanev, M. F. Decamp, and B. C. Walker, Electron Shell Ionization of Atoms with Classical, Relativistic Scattering, *Phys. Rev. Lett.* **110**, 203003 (2013).
- [54] M. C. Kohler, T. Pfeifer, K. Z. Hatsagortsyan, and C. H. Keitel, Electron correlation and interference effects in strong-field processes, *Adv. At. Mol. Phys.* **61**, 159 (2012).
- [55] C. J. Joachain and N. J. Kylstra, Relativistic effects in the multiphoton ionization of hydrogenlike ions by ultrashort infrared laser pulses, *Phys. Rev. A* **100**, 013417 (2019).
- [56] L. V. Keldysh, Ionization in the field of a strong electromagnetic wave, *Zh. Eksp. Teor. Fiz.* **47**, 1945 (1964) [*Sov. Phys. JETP* **20**, 1307 (1965)].
- [57] F. H. M. Faisal, Multiple absorption of laser photons by atoms, *J. Phys. B* **6**, L89 (1973).
- [58] H. R. Reiss, Effect of an intense electromagnetic field on a weakly bound system, *Phys. Rev. A* **22**, 1786 (1980).
- [59] A. M. Perelomov and V. S. Popov, Ionization of atoms in an alternating electric field, *Zh. Eksp. Teor. Fiz.* **50**, 1393 (1966) [*Sov. Phys. JETP* **23**, 924 (1966)].
- [60] V. S. Popov, Tunnel and multiphoton ionization of atoms and ions in a strong laser field (Keldysh theory), *Phys. Usp.* **47**, 855 (2004).
- [61] H. R. Reiss, Complete Keldysh theory and its limiting cases, *Phys. Rev. A* **42**, 1476 (1990).
- [62] H. R. Reiss, Relativistic strong-field photoionization, *J. Opt. Soc. Am. B* **7**, 574 (1990).
- [63] V. Popov, V. Mur, and B. Karnakov, The imaginary-time method for relativistic problems, *JETP Lett.* **66**, 229 (1997).
- [64] V. Mur, B. Karnakov, and V. Popov, Relativistic version of the imaginary-time formalism, *J. Exp. Theor. Phys.* **87**, 433 (1998).
- [65] N. Milosevic, V. P. Krainov, and T. Brabec, Semiclassical Dirac Theory of Tunnel Ionization, *Phys. Rev. Lett.* **89**, 193001 (2002).
- [66] N. Milosevic, V. P. Krainov, and T. Brabec, Relativistic theory of tunnel ionization, *J. Phys. B: At. Mol. Opt. Phys.* **35**, 3515 (2002).
- [67] A. M. Perelomov and V. S. Popov, Ionization of atoms in an alternating electric field. III, *Zh. Eksp. Teor. Fiz.* **52**, 514 (1967) [*Sov. Phys. JETP* **25**, 336 (1967)].
- [68] M. V. Ammosov, N. B. Delone, and V. P. Krainov, Tunnel ionization of complex atoms and of atomic ions in an alternating electromagnetic field, *Zh. Eksp. Teor. Fiz.* **91**, 2008 (1986) [*Sov. Phys. JETP* **64**, 1191 (1986)].
- [69] V. S. Popov, V. P. Kuznetsov, and A. M. Perelomov, Quasi-classical approximation for nonstationary problems, *Zh. Eksp. Teor. Fiz.* **53**, 331 (1967) [*Sov. Phys. JETP* **26**, 222 (1968)].
- [70] D. M. Wolkow, On a class of solutions of the dirac equation, *Z. Phys.* **94**, 250 (1935).
- [71] M. Jain and N. Tzoar, Compton scattering in the presence of coherent electromagnetic radiation, *Phys. Rev. A* **18**, 538 (1978).
- [72] G. L. Yudin, S. Chelkowski, and A. D. Bandrauk, Coulomb continuum effects in molecular interference, *J. Phys. B: At. Mol. Opt. Phys.* **39**, L17 (2006).
- [73] F. H. M. Faisal, Strong-field *S*-matrix theory with final-state Coulomb interaction in all orders, *Phys. Rev. A* **94**, 031401(R) (2016).
- [74] O. Smirnova, M. Spanner, and M. Y. Ivanov, Coulomb and polarization effects in laser-assisted XUV ionization, *J. Phys. B: At. Mol. Opt. Phys.* **39**, S323 (2006).
- [75] J. I. Gersten and M. H. Mittleman, Eikonal theory of charged-particle scattering in the presence of a strong electromagnetic wave, *Phys. Rev. A* **12**, 1840 (1975).
- [76] V. P. Krainov, Ionization rates and energy and angular distributions at the barrier-suppression ionization of complex atoms and atomic ions, *J. Opt. Soc. Am. B* **14**, 425 (1997).
- [77] C. C. Chirilă and R. M. Potvliege, Low-order above-threshold ionization in intense few-cycle laser pulses, *Phys. Rev. A* **71**, 021402(R) (2005).
- [78] S. V. Popruzhenko, G. G. Paulus, and D. Bauer, Coulomb-corrected quantum trajectories in strong-field ionization, *Phys. Rev. A* **77**, 053409 (2008).
- [79] S. V. Popruzhenko and D. Bauer, Strong field approximation for systems with Coulomb interaction, *J. Mod. Opt.* **55**, 2573 (2008).
- [80] X.-Y. Lai, C. Poli, H. Schomerus, and C. Figueira de Morisson Faria, Influence of the Coulomb potential on above-threshold ionization: A quantum-orbit analysis beyond the strong-field approximation, *Phys. Rev. A* **92**, 043407 (2015).

- [81] A. S. Maxwell, A. Al-Jawahiry, T. Das, and C. F. d. M. Faria, Coulomb-corrected quantum interference in above-threshold ionization: Working towards multi-trajectory electron holography, *Phys. Rev. A* **96**, 023420 (2017).
- [82] M. Klaiber, J. Daněk, E. Yakaboylu, K. Z. Hatsagortsyan, and C. H. Keitel, Strong-field ionization via a high-order Coulomb-corrected strong-field approximation, *Phys. Rev. A* **95**, 023403 (2017).
- [83] M. Klaiber, E. Yakaboylu, and K. Z. Hatsagortsyan, Above-threshold ionization with highly charged ions in superstrong laser fields. I. Coulomb-corrected strong-field approximation, *Phys. Rev. A* **87**, 023417 (2013).
- [84] O. Smirnova, M. Spanner, and M. Ivanov, Analytical solutions for strong field-driven atomic and molecular one- and two-electron continua and applications to strong-field problems, *Phys. Rev. A* **77**, 033407 (2008).
- [85] L. Torlina and O. Smirnova, Time-dependent analytical *R*-matrix approach for strong-field dynamics. I. One-electron systems, *Phys. Rev. A* **86**, 043408 (2012).
- [86] L. Torlina, J. Kaushal, and O. Smirnova, Time-resolving electron-core dynamics during strong-field ionization in circularly polarized fields, *Phys. Rev. A* **88**, 053403 (2013).
- [87] J. Kaushal and O. Smirnova, Nonadiabatic Coulomb effects in strong-field ionization in circularly polarized laser fields, *Phys. Rev. A* **88**, 013421 (2013).
- [88] T. Keil, S. V. Popruzhenko, and D. Bauer, Laser-Driven Recollisions under the Coulomb Barrier, *Phys. Rev. Lett.* **117**, 243003 (2016).
- [89] S. Palaniyappan, I. Ghebregziabher, A. DiChiara, J. MacDonald, and B. C. Walker, Emergence from nonrelativistic strong-field rescattering to ultrastrong-field laser-atom physics: A semiclassical analysis, *Phys. Rev. A* **74**, 033403 (2006).
- [90] H. K. Avetissian, K. Z. Hatsagortsyan, A. G. Markossian, and S. V. Movsissian, Generalized eikonal wave function of a Dirac particle interacting with an arbitrary potential and radiation fields, *Phys. Rev. A* **59**, 549 (1999).
- [91] H. K. Avetissian, A. G. Markossian, and G. F. Mkrtchian, Relativistic theory of the above-threshold multiphoton ionization of hydrogenlike atoms in ultrastrong laser fields, *Phys. Rev. A* **64**, 053404 (2001).
- [92] M. Klaiber, E. Yakaboylu, and K. Z. Hatsagortsyan, Above-threshold ionization with highly charged ions in superstrong laser fields. II. relativistic Coulomb-corrected strong-field approximation, *Phys. Rev. A* **87**, 023418 (2013).
- [93] S. X. Hu and C. H. Keitel, Spin Signatures in Intense Laser-Ion Interaction, *Phys. Rev. Lett.* **83**, 4709 (1999).
- [94] M. Casu, C. Szymanowski, S. Hu, and C. H. Keitel, Coherent x-ray generation with laser driven ions, *J. Phys. B: At. Mol. Opt. Phys.* **33**, L411 (2000).
- [95] C. H. Keitel and S. X. Hu, Coherent x-ray pulse generation in the sub-Ångström regime, *Appl. Phys. Lett.* **80**, 541 (2002).
- [96] M. W. Walser, D. J. Urbach, K. Z. Hatsagortsyan, S. X. Hu, and C. H. Keitel, Spin and radiation in intense laser fields, *Phys. Rev. A* **65**, 043410 (2002).
- [97] G. R. Mocken and C. H. Keitel, Bound atomic dynamics in the MeV regime, *J. Phys. B: At. Mol. Opt. Phys.* **37**, L275 (2004).
- [98] G. Mocken and C. H. Keitel, FFT-split-operator code for solving the Dirac equation in 2+1 dimensions, *Comput. Phys. Commun.* **178**, 868 (2008).
- [99] H. G. Hetzheim and C. H. Keitel, Ionization Dynamics versus Laser Intensity in Laser-Driven Multiply Charged Ions, *Phys. Rev. Lett.* **102**, 083003 (2009).
- [100] S. Selstø, E. Lindroth, and J. Bengtsson, Solution of the Dirac equation for hydrogenlike systems exposed to intense electromagnetic pulses, *Phys. Rev. A* **79**, 043418 (2009).
- [101] Y. V. Vanne and A. Saenz, Solution of the time-dependent Dirac equation for multiphoton ionization of highly charged hydrogenlike ions, *Phys. Rev. A* **85**, 033411 (2012).
- [102] F. Fillion-Gourdeau, E. Lorin, and A. D. Bandrauk, Numerical solution of the time-dependent Dirac equation in coordinate space without fermion-doubling *Comput. Phys. Commun.* **183**, 1403 (2012).
- [103] T. Kjellsson, S. Selstø, and E. Lindroth, Relativistic ionization dynamics for a hydrogen atom exposed to superintense XUV laser pulses, *Phys. Rev. A* **95**, 043403 (2017).
- [104] B. Hafizi, D. F. Gordon, and J. P. Palastro, First Benchmark of Relativistic Photoionization Theories against 3D *ab initio* Simulation, *Phys. Rev. Lett.* **118**, 133201 (2017).
- [105] D. A. Telnov and Shih-I. Chu, Relativistic ionization dynamics of hydrogenlike ions in strong electromagnetic fields: Generalized pseudospectral method for the time-dependent Dirac equation, *Phys. Rev. A* **102**, 063109 (2020).
- [106] P.-L. He, M. Klaiber, K. Z. Hatsagortsyan, and C. H. Keitel, High-energy direct photoelectron spectroscopy in strong-field ionization, *Phys. Rev. A* **98**, 053428 (2018).
- [107] W. Becker, F. Grasbon, R. Kopold, D. B. Milošević, G. G. Paulus, and H. Walther, Above-threshold ionization: From classical features to quantum effects, *Adv. Atom. Mol. Opt. Phys.* **48**, 35 (2002).
- [108] G. F. Gribakin and M. Y. Kuchiev, Multiphoton detachment of electrons from negative ions, *Phys. Rev. A* **55**, 3760 (1997).
- [109] M. Klaiber, E. Yakaboylu, C. Müller, H. Bauke, G. G. Paulus, and K. Z. Hatsagortsyan, Spin dynamics in relativistic ionization with highly charged ions in super-strong laser fields, *J. Phys. B: At. Mol. Opt. Phys.* **47**, 065603 (2014).